

# Online Radiation Dose Measurement System for ATLAS experiment

I. Mandić, V. Cindro, I. Dolenc, A. Gorišek, G. Kramberger, M. Mikuž, J. Hartert, J. Bronner, S. Franz

**Abstract**— In experiments at Large Hadron Collider detectors and electronics will be exposed to high fluxes of photons, charged particles and neutrons. Damage caused by the radiation will influence performance of detectors. It will therefore be important to continuously monitor the radiation dose in order to follow the level of degradation of detectors and electronics and to correctly predict future radiation damage. A system for online radiation monitoring using semiconductor radiation sensors at large number of locations has been installed in the ATLAS experiment. Ionizing dose in SiO<sub>2</sub> will be measured with RadFETs, displacement damage in silicon in units of 1-MeV(Si) equivalent neutron fluence with *p-i-n* diodes. At 14 monitoring locations where highest radiation levels are expected the fluence of thermal neutrons will be measured from current gain degradation in dedicated bipolar transistors. The design of the system and tests of its performance in mixed radiation field is described in this paper.

**Index Terms**—Accelerators, dosimetry, *pin* diodes, RadFET, radiation damage

## I. INTRODUCTION

Detectors and readout electronics in the high energy physics experiment ATLAS at the Large Hadron Collider at CERN [1],[2] will be exposed to high levels of radiation. The radiation field will contain photons, charged particles and neutrons. The particles in the radiation field will originate from proton-proton interactions as well as from interactions of secondary particles with material in the experimental apparatus. The radiation will cause damage to detector equipment so it will be important to monitor the accumulated doses during detector operation. Although detailed simulations of the radiation field were made, a monitoring system is needed to verify the simulations, to optimize the operation scenario and to correctly predict the lifetime of radiation sensitive components of experimental equipment.

I. Mandić, V. Cindro, I. Dolenc, A. Gorišek, G. Kramberger and M. Mikuž are with the Jožef Stefan Institute, Jamova 39, Ljubljana, Slovenia (telephone: (+386)1 4773535, e-mail: [Igor.Mandic@ijs.si](mailto:Igor.Mandic@ijs.si)).

M. Mikuž is also with the Faculty of Mathematics and Physics, University of Ljubljana, Slovenia.

J. Hartert and J. Bronner are with Physikalisches Institut Universität Freiburg, Hermann-Herder-Str. 3, Freiburg, Germany.

S. Franz is with CERN, Geneva, Switzerland.

ATLAS is a large cylindrically shaped apparatus with

radius of about 13 m and length of about 46 m. The proton-proton interaction point is in the centre of the cylinder. In the innermost parts of ATLAS detector, during 10 years of operation, certain electronic components will be exposed to over 100 kGy of ionizing dose and will suffer bulk damage as caused by fluence of the order of  $10^{15}$  1 MeV-equivalent neutrons (in Si) per cm<sup>2</sup> [3]. Radiation monitors must therefore be capable of measuring such doses. At the same time, the sensitivity of radiation monitors must be sufficient to give information about the radiation field already in the early stage of experiment in order to cross-check the simulations as soon as possible.

Further away from the interaction point lower radiation levels are expected. However, uncertainties of simulations at these locations are larger and the purpose of radiation monitoring at those locations is to detect if electronics or other radiation sensitive detector components are exposed to excessive doses.

## II. DESCRIPTION OF THE SYSTEM

In the monitoring system in ATLAS experiment various semiconductor sensors are used to measure integrated radiation doses. Choice of silicon sensors is natural in the environment with stringent space constraint because of their small size. At the same time the damage to the readout electronics and silicon detectors is easiest followed with these sensors because the radiation effect exploited for monitoring is the same as the effect that causes damage in detectors and electronics.

The basic unit of the system is a Radiation Monitor Sensor Board (RMSB) which hosts radiation detectors that can be read-out online. In the innermost part of ATLAS detector (called Inner Detector – ID [4]) RMSBs are placed at 14 locations and provide on-line information of ionization dose in SiO<sub>2</sub> and NIEL in silicon. They also enable measurements of gain degradation in the dedicated npn bipolar transistors which are used also in the readout chips of ATAS silicon strip detector. The fluence of thermal neutrons can be estimated from gain degradation in

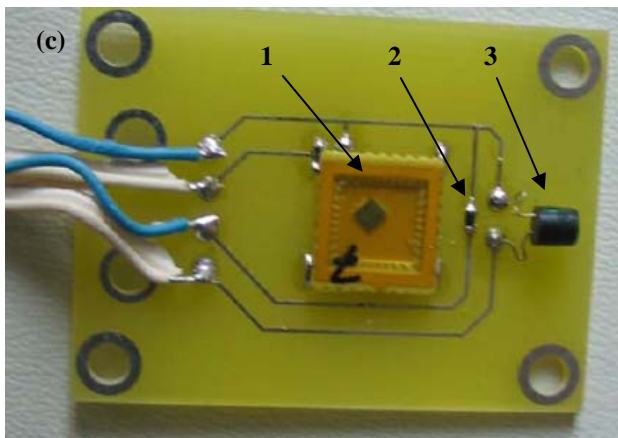
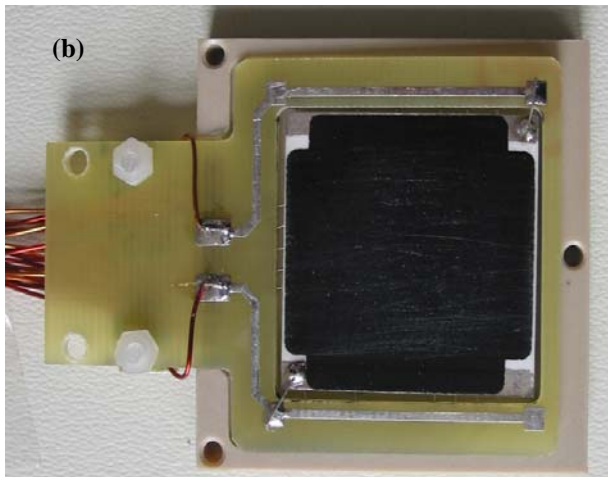
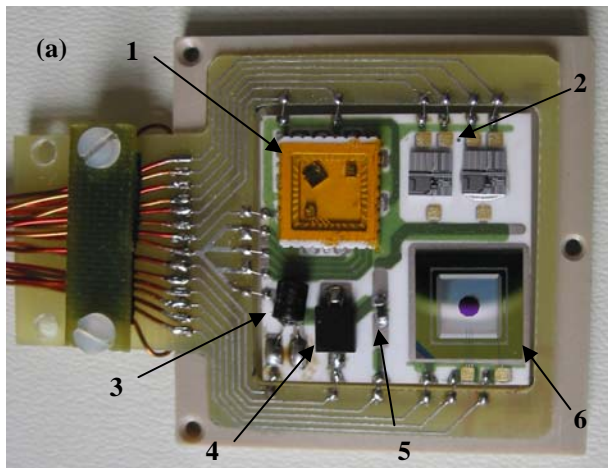


Fig. 1. Photo of populated Inner Detector RMSB (a). Ceramic hybrid with sensors is connected to a PCB frame. In the upper left corner there is a package with 3 RadFETs (arrow 1) and next to it there are 2 DMILL test structures (arrow 2). Under the RadFET package are CMRP (arrow 3) and BPW34 (arrow 4) diodes. Next to the diodes is the temperature sensor (arrow 5). In the lower right corner the pad diode (arrow 6) can be seen. The back side of the hybrid is shown in (b). The ceramic is covered with a thick-film resistive layer ( $R = 320 \Omega$ ), which serves as heater. Dimensions of the box which supports the PCB frame on the photo are 4 cm x 4 cm. Figure (c) shows the simplified RMSB used in locations outside of the ID. A RadFET package containing only the high sensitivity sensor (1), temperature sensor (2) and a CMRP diode (3) can be seen. The dimensions of the PCB are 4 cm x 3 cm.

these transistors [5]. In the Inner Detector there will be no access to the RMSBs during 10 years of operation. So they host a number of radiation detectors which cover large dose range and also provide a high level of redundancy (see Fig. 1).

The locations of monitors in the ID can be seen in Fig. 2. The locations were chosen to get monitoring points uniformly distributed around Inner Detector but the choice of locations was driven mainly by space limitations.

Simplified version of RMSBs, covering lower dose ranges, are installed at 48 locations outside of the Inner Detector, i.e. at larger distances from the interaction point, near radiation sensitive electronic equipment.

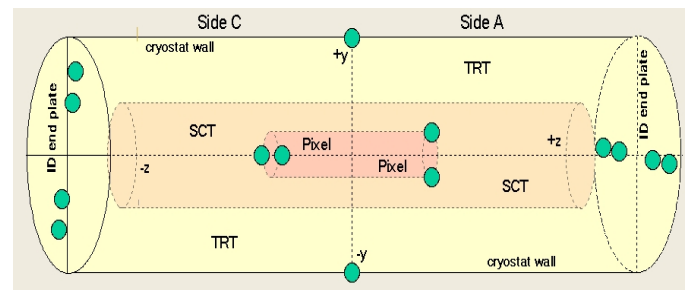


Fig 2. Scheme of the Inner Detector with 14 locations of radiation monitors marked with green symbols. Inner Detector consists of three subsystems: Pixel detector, Semi-Conductor Tracker (SCT) and Transition Radiation Tracker (TRT). The length of the Inner Detector is  $\sim 7$  m and radius  $\sim 1$  m. The interaction point is in the center of the cylinder.

### A. RADIATION SENSORS

There are three types of radiation sensors, sensitive to different radiation types, used in the system.

#### 1) Total Ionizing Dose

The on-line measurement of the Total Ionizing Dose (TID) is done with radiation sensitive p-MOS transistors (RADFETs) in which dose is measured from the increase of the gate voltage at a given drain current [6]. To cover the required dynamic range, 3 RADFETs with different oxide thickness are placed on each RMSB in the ID: high sensitivity ( $1.6 \mu\text{m}$  oxide thickness, mGy sensitivity, up to 10 Gy total dose produced by LAAS, Toulouse, France [7]), intermediate ( $0.25 \mu\text{m}$  oxide thickness from REM [8], up to tens of kGy) and low sensitivity ( $0.13 \mu\text{m}$  oxide thickness, REM, up to  $10^5$  kGy). Only most sensitive RADFETs (LAAS) are used on RMSBs outside of the ID.

The relation of absorbed dose  $D$  to gate voltage increase  $\Delta V$  varies between types of RadFETs and must be determined experimentally. It can be approximated with:  $D = a(\Delta V)^b$ , where  $a$  and  $b$  are calibration constants which must be determined for each type and production batch of RadFETs [9],[10]. The measurement is done so that gate and drain contacts are at the same potential and gate voltage is measured relative to the source/bulk contact at a given drain current. The drain current is  $I_d = 100 \mu\text{A}$  for LAAS RadFET and  $I_d =$

160  $\mu\text{A}$  for REM RadFETs. At these values of drain current minimal dependence of gate voltage on temperature is achieved.

## 2) Bulk Damage

Bulk damage in silicon is monitored with diodes using two different measurement methods: measurement of leakage current in a reverse biased diode and measurement of forward diode voltage at given forward current. The leakage current increase in reverse biased diode ( $\Delta I$ ) after irradiation is directly proportional to Non-Ionizing Energy Loss (NIEL). The 1 MeV neutron equivalent fluence ( $\Phi_{eq}$ ) is determined from  $\Phi_{eq} = \Delta I / (\alpha(t, T) \cdot V)$ , where  $\alpha(t, T)$  is the leakage current damage constant and  $V$  the sensitive (i.e. depleted) volume of the diode. The constant  $\alpha(t, T)$  is a well measured quantity, independent of type of silicon material and with well known temperature and annealing behavior [11],[12]. In this measurement method it is necessary that the diode is fully depleted during the whole life of experiment i.e. also at fluences exceeding  $10^{14}$  n/cm<sup>2</sup>. Since the highest voltage supplied to the system is 30 V, special pad-detector diodes with only 25  $\mu\text{m}$  active thickness processed on epitaxial silicon of 50  $\Omega\text{cm}$  at CiS, Erfurt, Germany [13] are used. An important feature of epitaxial diodes is that the full-depletion voltage does not increase with annealing time [14] - in time scales and fluence ranges considered here. The diodes have a 0.5 cm x 0.5 cm active area and a guard ring structure.

Two diodes per RMSB in the ID are used for measurements of bulk damage in silicon from increase of forward voltage at given forward current - 1 mA in our case. Displacement damage in silicon causes degradation of minority carrier lifetime and increase of material resistance. The consequence of this is that the forward bias voltage needed to drive a given current through the diode increases with irradiation [15]. It has been shown in [16] that a commercial silicon pin photodiode (OSRAM - BPW34F) [17] can be used to measure NIEL equivalent fluence in the range from  $5 \cdot 10^{12}$  n/cm<sup>2</sup> to  $10^{14}$  n/cm<sup>2</sup>. The response to radiation at lower fluences is strongly non-linear. However, the sensitivity and linear regime at low fluences can be improved by pre-irradiating the diodes. The BPW34F diodes used in ATLAS have been pre-irradiated with  $3 \times 10^{12}$  n/cm<sup>2</sup> (1 MeV neutrons NIEL equivalent).

Sensitivity to radiation increases with the width of intrinsic base. Lower fluences, in the range from  $10^9$  to  $5 \times 10^{12}$  n/cm<sup>2</sup>, are covered with more sensitive silicon PIN diodes with about 1 mm base width from CMRP, Wollongong Australia. Also in these diodes the 1 MeV neutron NIEL equivalent in silicon is measured by measuring voltage at 1 mA forward current.

In both diodes the 1 MeV neutron equivalent fluence  $\Phi_{eq}$  is calculated from linear relation :  $\Phi_{eq} = k \cdot \Delta V$ , where  $\Delta V$  is the forward voltage increase and  $k$  is the constant determined from calibration irradiations. For the BPW34 diode the value of the constant is  $k = 1 \cdot 10^{13}$  ncm<sup>-2</sup>/V [18] and for CMRP diodes  $k = 1.7 \cdot 10^{11}$  ncm<sup>-2</sup>/V [9]. The accuracy if calibration

constants is about 15%.

## 3) Thermal Neutrons

In the npn DMILL bipolar transistors the common emitter current gain factor  $\beta = I_c / I_b$  (collector current/base current) is measured at collector current  $I_c = 10 \mu\text{A}$ . The degradation of  $\beta$  is the major reason for degradation of ASIC performance [19] so it is important to monitor the condition of transistors, to understand the performance of readout electronics. In addition, it is a feature of these transistors, that their  $\beta$  degrades substantially also when irradiated with thermal neutrons so they can be used to monitor fluences of thermal neutrons larger than few times  $10^{12}$  n/cm<sup>2</sup> [5],[18].

Beta degradation in these transistors is caused by both, fast and thermal neutrons. It was shown in [5] that the contribution of the two degradations is additive and can be written as

$$\frac{\Delta I_b}{I_c} = k_{eq} \cdot \Phi_{eq} + k_{th} \cdot \Phi_{th} \quad (1)$$

where  $k_{eq}$  and  $k_{th}$  are the equivalent and thermal neutron damage factors, respectively. Since the 1 MeV equivalent fluence  $\Phi_{eq}$  is known from measurements with diodes, the measurement of base current increase  $\Delta I_b$  provides information about the thermal neutron fluence  $\Phi_{th}$ .

## B. RMSB Hybrid

The Inner detector RMSB hosts three RadFETs, a CMRP diode, a BPW34 diode, an epitaxial pad diode, two DMILL test structures and a temperature sensor (10 k $\Omega$  NTC). A 0.6 mm thick, Al<sub>2</sub>O<sub>3</sub> hybrid provides mechanical support and electrical connections for the sensors. Fig. 1(a) shows a hybrid populated with sensors and mounted in a PCB frame. The frame with the hybrid is placed in a housing made of PEEK plastic to mechanically protect the sensors and provide an air gap for thermal insulation. The outer dimensions of the housing are 4 cm x 4 cm x 0.8 cm.

At certain proposed locations of the radiation monitors in the Inner Detector the temperature conditions are not precisely known and could vary between -20° and +20° C. To stabilize the temperature of all sensor boards to approximately +20° C the back side of the hybrid is covered with a thick-film resistive layer ( $R = 320 \Omega$ ) which serves as a heater (see Fig. 1(b)).

Fig. 1(c) shows the simplified version of RMSB used in locations outside of the ID. The RMSB is a standard PCB equipped with a package containing only the high sensitivity RadFET, temperature sensor and the CMRP diode.

## III. READOUT AND INTEGRATION IN ATLAS

Readout of sensors is done online with standard ATLAS detector control system (DCS) hardware components. Usage of these components ensures full compatibility and simplifies integration of the radiation monitor into DCS. The main

readout component is the Embedded Local Monitor Board (ELMB) [20] which hosts 64 16-bit ADC channels (0 - 5 V) with the conversion frequency ranging from 2-100 Hz. The current sources for sensor readout are 16 channel 12-bit DAC boards controlled by the ELMB. Up to four DAC board can be connected to each ELMB. The output from the ELMB-DAC is a current, with a maximum of 20 mA per channel. The maximum output voltage of a DAC channel is 30 V.

The radiation sensors read out procedure is composed of the following steps: apply current to the sensor (bias resistor in the case of reverse biased diode) with DAC - wait - read out voltage on sensor (resistor) using ADC - bias off. The length of the wait step is set individually for each sensor in the range from 500 ms for CMRP and BPW34 diodes, to 3 seconds for epi-diodes. Constant current is enforced through the temperature sensor, and the voltage on the sensor is read by an ADC channel during the readout cycle. The readout cycle is launched few times per hour.

Each RMSB is connected to the box containing ELMB, DAC and patch panel boards. Patch panel board interfaces DACs and ADCs to the sensors. It also hosts measurement resistors, voltage attenuators (to enable measurements of voltages higher than 5 V which is the maximum for ADCs on ELMB), and over-voltage protection circuits for transistors. Sensors are biased only during the read out process and this time is short compared to the exposure time. During exposure sensor contacts are shorted via J-FET transistors (2N5461) mounted on the patch panel board and connected in parallel to the sensors. When the J-FET is not biased the resistance between source and drain is  $\sim 300$  Ohms. During readout one DAC channel sets the bias to the gates of the J-FET transistors and so disconnects the conduction path parallel to the sensors.

In the Inner Detector the RMSBs are connected over about 18 m long cables to readout boxes. Each RMSB has its own DAC board and two RMSBs are read out by one ELMB. Outside of the Inner Detector the length of cables varies. The maximal cable length which was tested was 200 m. Up to 12 RMSBs are connected to a readout box containing one ELMB and 2 DAC and patch-panel boards.

In the Inner Detector where RMSBs are equipped with the heater (see Fig. 1b), four DAC channels in parallel are used as power source of the hybrid heater. The temperature stabilization program runs on the ELMB processor. It sets the heater current from DAC based on the measured difference between actual and desired temperature on the RMSB. Four DAC channels provide maximum power of about 2 W which is sufficient to maintain temperature of RMSB about 40°C above the ambient temperature. The system is able to stabilize temperature to better than 1°C.

The simplified version of RMSBs in locations outside of the Inner Detector do not have the temperature stabilization feature because the ambient temperature at those locations is better defined. The effect of temperature on dose measurements is taken into account already in the online processing of readout values using known dependences for each type of sensors.

Communication between the computer that runs the DCS software and the ELMBs is done via CANbus. The computers as well as power supplies for ELMB and DAC boards are located outside of the detector area so that they are not exposed to radiation and can be accessed also during data-taking. The cables connecting computer and power supplies with readout boxes are up to 100 m long. The radiation monitor application is written in PVSS [21], a commercial SCADA software that is used by all LHC experiments. The application runs as a client of an OPC server which communicates with the hardware. The status of the readout electronics and the online values of the RMSBs are collected in a single control application which is included in the common infrastructure control of ATLAS. User interfaces are provided in the ATLAS control room and all values are archived and made available for offline analysis. After significant doses will be accumulated, the detailed analysis of archived data will allow a precise validation of simulations. Correlation between doses and accelerator luminosity will be determined which will allow to make predictions of radiation damage in detector components.

The system was completely installed and the readout software integrated in the frame of ATLAS DCS software in the year 2008. All the RMSBs have been readout during several months before the operation of ATLAS started. The stability of the readout has been proven and temperature correction factors have been calculated using these data in order to correct the raw values of the RMSBs during the operation. It was discovered that responses of BPW34 and CMRP diodes are influenced by the strong magnetic field in the ATLAS detector. Detailed studies of this effect showed that it can be controlled and does not represent an obstacle to the performance of the system.

More details about design and performance of the system can be found in references [12],[18],[22].

#### IV. TESTS IN MIXED PARTICLE ENVIRONMENT

Inner Detector type of RMSBs, read-out with the same components as used in the final system, were installed in the low-dose-rate mixed-particle environment in the CERN – IRRAD6 facility [23],[24]. In the CERN irradiation facility 23 GeV proton beam is directed towards the marble absorber placed in front of a cast iron beam dump. The primary proton interactions in the absorber and beam dump produce a radiation field composed of neutrons, photons, pions and protons in the surrounding. This environment is called IRRAD6. The mixed particle, low-rate accelerator environment in the IRRAD6 with runs of variable intensity with shut downs simulates well the expected working conditions in the LHC.

The number of protons delivered to the irradiation facility is measured with a Secondary Emission Counter – SEC. Using different means of dozimetry it is possible to correlate the SEC counter with the dose delivered to the RMSBs in the IRRAD6. The RMSBs were installed in the IRRAD6 in the

summer of 2008. The sensors were read out few times per hour. Temperature varied by about 5°C around 25°. The temperature measurements were also recorded and the sensor readout values were corrected for temperature effects.

### A. Measurements with RadFETS

Total dose of  $410 \pm 20$  Gy at the location of RMSBs after the end of irradiation period in November 2008 was measured with alanine dosimeter. This value was used to convert SEC counts to Gy. Fig 3 shows TID measured with RadFETs on RMSBs as a function of time. Fig. 3(a) shows measurements taken with the high sensitivity LAAS RadFET at the

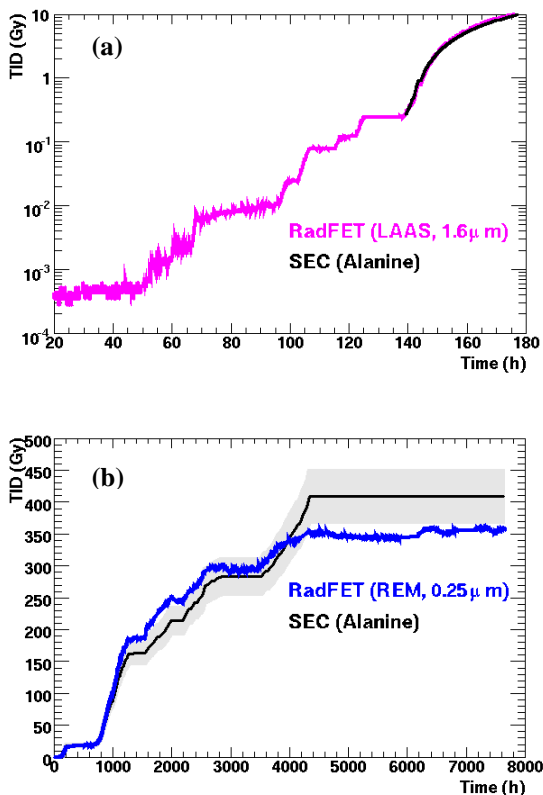


Fig 3. (a) TID measured with high sensitivity LAAS RadFET in the beginning of the data taking. The sensitivity better than mGy can be seen. Good agreement with expected dose based on measurements with SEC counter can be seen. Fig (b) shows measurements with intermediate dose RadFET (with 0.25 μm oxide thickness) compared to SEC counter over the entire data taking period. The shaded area represents the uncertainty of SEC calibration. beginning of irradiation season. It can be seen that doses of the order of mGy can be measured. The comparison with SEC counter is shown at times larger than 140 hours after the start because the SEC values are too uncertain at the start of irradiation period due to beam tuning. However, the steps of dose increases measured with RadFET can be correlated with beam on and off times. LAAS RadFET can be used up to total dose of about 10 Gy after which its response saturates [9].

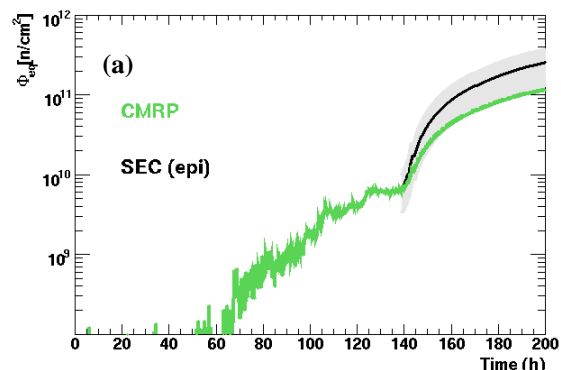
Larger doses are measured with REM RadFETs with thinner oxide layer. Fig 3(b) shows measurements with intermediate-range RadFET (with 0.25 μm oxide thickness) compared to SEC counter over the entire data taking period.

Good agreement with expected dose profile can be seen. From the SEC profile it can be seen that the end of beam time started at Time ~ 4000 hours. It is important to note that no significant annealing of RadFET response is observed during the next 4000 hours without beam.

### B. Measurements with diodes

Bulk damage in silicon is measured with diodes as explained above. The 1 MeV neutron fluence NIEL equivalent in silicon ( $\Phi_{eq}$ ), measured with epi-diode on the RMSB was used to normalize the SEC counter. The reverse current of  $I = 0.11$  μA was measured in the epi diode at the end of test period (at Time = 8000 h). After 4000 hours without beam and 8000 hours since start of experiment, at temperature of about 20°C, a good approximation for leakage current damage constant is  $\alpha = 2.7 \cdot 10^{-17}$  Acm [12]. The volume of the diode is  $V = 0.5^2 \times 0.0025$  cm<sup>3</sup> =  $6.25 \cdot 10^{-4}$  cm<sup>3</sup>. From these numbers the fluence can be calculated:  $\Phi_{eq} = I/(V\alpha) = 6.5 \cdot 10^{12}$  n/cm<sup>2</sup> with uncertainty of about 20%. This number is used to convert SEC counts to  $\Phi_{eq}$ .

Fig 4. shows the 1 MeV neutron equivalent fluence measured with diodes. Fig 4(a) shows the measurements made with high sensitivity CMRP diode at the start of experiment. From this figure it can be seen that equivalent fluences as small as 10<sup>9</sup> n/cm<sup>2</sup> can be measured. In Fig 4(b) measurements of equivalent fluences with three different diodes are shown without correcting the responses of diodes for annealing effects i.e. measured currents and voltages are converted to fluence by multiplying them with appropriate conversion constants.



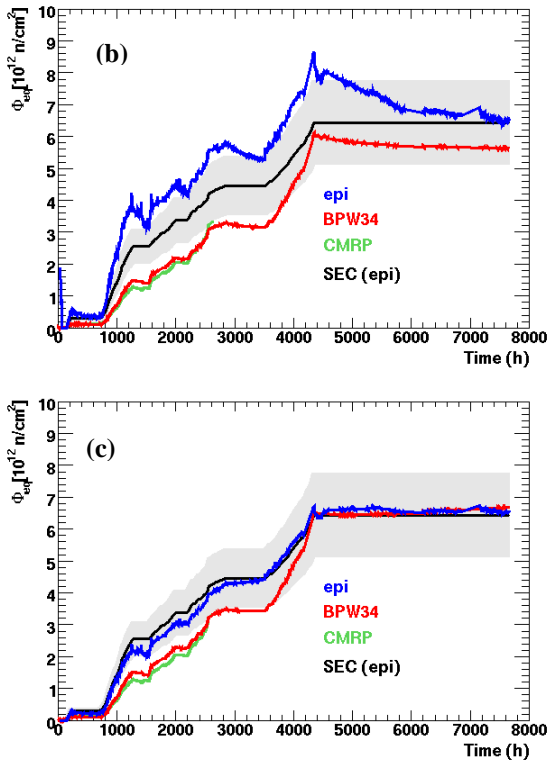


Fig 4. Measurements of 1 MeV neutron equivalent fluences. Figure (a) shows the fluence measured with high sensitivity CMRP diode. In figure (b) measurements with three different diodes over the entire irradiation period are shown before correction for annealing effects. In figure (c) the measurements with epi and BPW34 have been corrected for annealing. The SEC counter was normalized with measurements with epi-diode at the end of irradiation (at Time = 8000 h) and the shaded area represents the 20% uncertainty of the normalization.

Measurements of long term annealing effects have been performed [12],[24],[25]. It was found that the annealing effects are significant for this application only for epi and BPW34 diodes. For these two sensors the annealing phenomena can be approximated by a stable value of current (voltage) after an exponential decay. For increase of reverse current  $I$  after irradiation with fluence  $\Phi$  in the epi diode it can therefore be written:

$$I(t) = I_1(t) + I_0 \quad (2)$$

$$I_1(t) = V\Phi\alpha_1 \cdot e^{-\frac{t}{\tau}}; \quad I_0 = V\Phi\alpha_0 \quad (3)$$

$$\frac{dI(t)}{dt} = -\frac{I_1(t)}{\tau} \quad (4)$$

Where  $V$  is the diode volume,  $dI(t)/dt$ ,  $\alpha_1$  and  $\tau$  are the annealing parameters. Change of current  $\Delta I$  measured in the diode on the RMSB, after time interval  $\Delta t$ , during which it was irradiated with fluence  $\Delta\Phi$  can be written as:

$$\Delta I = \alpha V \Delta\Phi - \frac{dI(t)}{dt} \cdot \Delta t = \alpha V \Delta\Phi - \frac{I_1(t)}{\tau} \cdot \Delta t, \quad (5)$$

where  $\alpha = \alpha_1 + \alpha_0$ . From measured change of current the fluence of this step can be calculated:

$$\Delta\Phi = \frac{1}{\alpha V} \left( \Delta I + \frac{I_1(t)}{\tau} \cdot \Delta t \right). \quad (6)$$

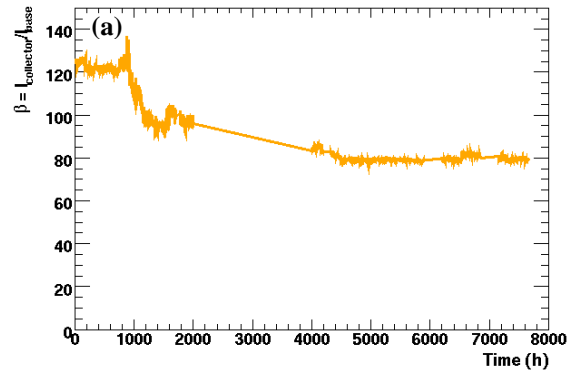
Similar calculations can be done also for the response of BPW34 diode. Annealing parameters are obtained from long term annealing measurements [12].

In Fig 4(c) measurements are shown after annealing of leakage current in case of epi and forward voltage for BPW34 diodes have been taken into account. One can see in Fig 4(c) that fluence measured with epi-diode follows the shape of SEC counter very well over the entire irradiation period. Measurements with BPW and CMRP diodes show somewhat lower response compared to epi-diode. But it should be mentioned that in the range of fluences below  $5 \cdot 10^{12} \text{ n/cm}^2$  the response of BPW34 diode could deviate from linearity even if it was pre-irradiated with  $3 \cdot 10^{12} \text{ n/cm}^2$ . In the case of CMRP the source of disagreement could be uncertainties of calibration constants which are of the order of 15% and annealing which contributes another 15%. It should also be mentioned that SEC counter has been normalized with measurement with epi-diode at the end of irradiation period and the uncertainty of extrapolation to lower fluences might be larger than shown in Fig. 4 by the shaded area.

### C. Measurements with transistors

From measurements with bipolar transistors degradation of common emitter current gain factor  $\beta$  is monitored. In Fig 5(a) the evolution of  $\beta$  measured at collector current  $I_c = 10 \mu\text{A}$  is shown. Values between Time = 2000 h and Time = 4000 h are missing because of problems with readout.

The fluence of thermal neutrons calculated from  $\beta$  degradation as explained above is shown in Fig 5(b). It can be seen that fluences of few times  $10^{12} \text{ n/cm}^2$  can be measured.



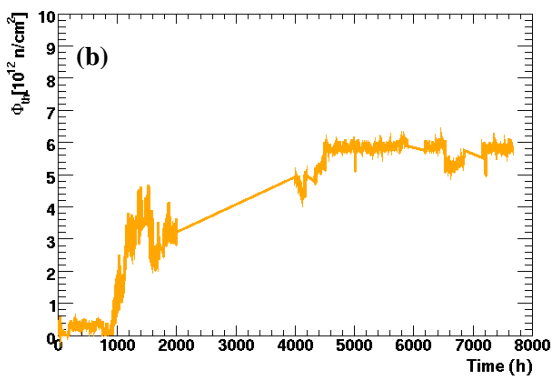


Fig 5. Measurements with bipolar transistors. Figure (a) shows measurements of common-emitter current gain  $\beta$  measured at collector current of 10  $\mu$ A. Figure (b) shows thermal neutron fluence calculated from  $\beta$  degradation. Values between Time = 2000 h and 4000 h are missing because of the readout problems.

## V. CONCLUSIONS

Online integrating radiation dose monitoring system for ATLAS detector was fully installed and integrated into detector control system of the ATLAS experiment in the year 2008. Radiation doses are measured with silicon sensors. TID is measured with RadFETs and NIEL is measured with diodes. Monitor boards with radiation sensors are installed at 14 locations in the Inner Detector and at 48 locations at greater radii. Monitors in the Inner Detector are equipped with larger number of sensors in order to cover larger range of doses.

The sensors installed in the final system in experimental cavern have been read out for several months. Good stability of the system was confirmed. The radiation monitor is ready for first measurements of radiation doses caused by proton-proton interactions in the ATLAS detector.

Inner Detector type of sensor boards were installed in the IRRAD6 facility at CERN in the long-term irradiation test. The radiation environment in the IRRAD6 simulates the running condition in the LHC and the system has been taking data for the last 11 months. First results from this test campaign confirm that doses can be measured with sufficient sensitivity (mGy for TID measurements,  $10^9$  n/cm<sup>2</sup> for NIEL measurements,  $10^{12}$  n/cm<sup>2</sup> for thermal neutrons) and accuracy (about 20 %) for usage in the ATLAS detector. It was shown that annealing phenomena which are important in final application and can be studied in a long-term irradiation experiment, can be taken into account with sufficient accuracy.

## ACKNOWLEDGMENT

The authors would like to thank Maurice Glaser and Federico Ravotti from CERN for all the help with irradiation test in the IRRAD6 and for many helpful advice and discussions which were of great importance for understanding the performance of radiation sensors and interpretation of collected data.

## REFERENCES

- [1] ATLAS Detector and Physics Performance Technical Design Report, CERN/LHCC/99-14/15 (1999).
- [2] The ATLAS collaboration, G. A. Aad et al., "The ATLAS Experiment at the CERN Large Hadron Collider", JINST, 2008 JINST 3 S08003
- [3] I. Dawson and C. Buttar, "The radiation environment in the ATLAS inner detector", *Nucl. Inst. Meth. A453*, pp. 461-467, 2000.
- [4] ATLAS TDR, Inner Detector Technical Design Report, CERN/LHCC/97-17, (1997).
- [5] I. Mandić, V. Cindro, G. Kramberger, E. S. Krištof, M. Mikuž, D. Vrtačnik, M. Ullán and F. Anghinolfi, "Bulk Damage in DMILL npn Bipolar Transistors Caused by Thermal Neutrons Versus Protons and Fast Neutrons", *IEEE Trans. Nucl. Sci.*, vol. 51, pp. 1752-1758, 2004.
- [6] A. G. Holmes-Siedle and L. Adams, "RadFETs: a review of the use of metal-oxide-silicon device as integrating dosimeters", *Rad. Phys. Chem.*, vol. 28, pp. 235-244, 1986.
- [7] G. Sarra Bayrouse, V. Polischuk, "MOS ionizing radiation dosimeters: from low to high dose measurements", *Rad. Phys. And Chem.*, vol. 61, pp- 511-513., 2001
- [8] Radiation Experiments and Monitors (REM) Webpage [Online]. Available: <http://www.radfet.com>
- [9] F. Ravotti, M. Glaser, M. Moll, "SENSOR CATALOGUE – Data Compilation of Solid-state Sensors for Radiation Monitoring", CERN TS.Note.2005-002, 13 May 2005.
- [10] F. Ravotti, M. Glaser, A.B. Rosenfeld, A.G. Holmes-Siedle and G. Sarra Bayrouse, "Radiation Monitoring in Mixed Environments at CERN: from the IRRAD6 Facility to the LHC Experiments", *IEEE Trans. Nucl. Sci.*, vol. 54, pp. 1170-1177, 2007.
- [11] M. Moll, E. Fretwurst, G. Lindström, "Leakage current of hadron irradiated silicon detectors - material dependence", *Nucl. Instr. and Meth A* 426 pp 87-93, 1999.
- [12] G. Kramberger, V. Cindro, I. Mandić, M. Mikuž, I. Dolenc, "Design and Functional Specification of ATLAS Radiation Monitor" ATL-IC-ES-0017
- [13] CiS Institut für Mikrosensorik gGmbH, Erfurt, Germany [Online]. Available: <http://www.cismst.de>
- [14] G. Lindström, I. Dolenc, E. Fretwurst, F. Hönniger, G. Kramberger, M. Moll, E. Nossarzewska, I. Pintilie and R. Röder, "Epitaxial silicon detectors for particle tracking—Radiation tolerance at extreme hadron fluences", *Nucl. Inst. Meth. A568*, pp. 66-71, 2006.
- [15] J. M. Swartz and M. O. Thurston, "Analysis of the Effect of Fast-Neutron Bombardment on the Current-Voltage Characteristic of a Conductivity-Modulated p-i-n Diode", *J. Appl. Phys.*, Vol. 37, (1966) pp 744.
- [16] M. Tavelt, M.E. Leon-Florian, "Dose and neutron-fluence measurements in mixed gamma-neutron fields by means of semiconductor dosimeters", *IEEE Catalogue RADECS '93, St. Malo, France, 1993*, pp. 27-32.
- [17] BPW34 photodiode datasheet. OSRAM Opto-Semiconductors [Online]. Available: <http://www.osram-os.com>
- [18] I. Mandić, V. Cindro, A. Gorišek, G. Kramberger and M. Mikuž, "Online Integrating Radiation Monitoring System for the ATLAS Detector at the Large Hadron Collider", *IEEE Trans. Nucl. Sci.*, vol. 54, pp. 1143-1150, 2007.

- [19] I. Mandić, "Radiation Effects in the Readout Chip for the ATLAS Semiconductor Tracker", *IEEE Trans. on Nucl. Sci.*, Vol. 49, no 6, pp. 2888-2894, Dec 2002.
- [20] H. Boternobrood, H.J. Burckhart, J. Cook, V. Filimonov, B. Hallgren, W. Heubers et al., "Design and implementation of the ATLAS detector control system", *IEEE Trans. Nucl. Sci.*, vol. 51, pp. 495-501, 2004.
- [21] PVSS is developed by ETM professional control GmbH [Online]. Available: <http://www.etm.at>
- [22] J. Hartert, J. Bronner, V. Cindro, A. Gorišek, G. Kramberger, I. Mandić, M. Mikuž, "The ATLAS Radiation Dose Measurement System and its Extension to SLHC", Proceedings of the Topical Workshop on Electronics for Particle Physics – TWEPP-08, Naxos, Greece. CERN-2008-08
- [23] F. Ravotti, M. Glaser, A. B. Rosenfeld, A.G. Holmes-Siedle and G. Sarrabayrouse, "Radiation Monitoring in Mixed Environment at CERN: from the IRRAD6 Facility to the LHC Experiments", *IEEE Trans. Nucl. Sci.*, vol. 54 (4), pp. 1170-1177, 2007.
- [24] F. Ravotti, "Development and Characterization of Radiation Monitoring Sensors for the High Energy Physics Experiments of the CERN LHC Accelerator", CERN-THESIS-2007-013.
- [25] F. Ravotti, M. Glaser, F. Saigné, L. Dusseau, G. Sarrabayrouse, "Prediction of the Thermal Annealing of Thick Oxide Metal-Oxide-Semiconductor Dosimeters Irradiated in a Harsh Radiation Environment", *Applied Physics Letters*, vol. 89 (8), article 083503, 3 pages, August 2006.